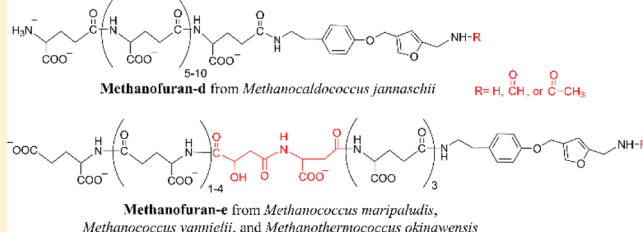


Identification of Structurally Diverse Methanofuran Coenzymes in Methanococcales That Are Both N-Formylated and N-Acetylated

Kylie D. Allen and Robert H. White*

Department of Biochemistry, Virginia Polytechnic Institute and State University, Blacksburg, Virginia 24061-0308, United States

ABSTRACT: Methanofuran (MF) is a coenzyme necessary for the first step of methanogenesis from CO_2 . The well-characterized MF core structure is 4-[N -(γ -L-glutamyl- γ -L-glutamyl)- p -(β -aminoethyl)phenoxyethyl]-2-(aminomethyl)furan (APMF- γ -Glu₂). Three different MF structures that differ on the basis of the composition of their side chains have been determined previously. Here, we use liquid chromatography coupled with high-resolution mass spectrometry and a variety of biochemical methods to deduce the unique structures of MFs present in four different methanogens in the order Methanococcales. This is the first detailed characterization of the MF occurring in methanogens of this order. MF in each of these organisms contains the expected APMF- γ -Glu₂; however, the composition of the side chain is different from that of the previously described MF structures. In *Methanocaldococcus jannaschii*, additional γ -linked glutamates that range from 7 to 12 residues are present. The MF coenzymes in *Methanococcus maripaludis*, *Methanococcus vannielii*, and *Methanothermococcus okinawensis* also have additional glutamate residues but interestingly also contain a completely different chemical moiety in the middle of the side chain that we have identified as *N*-(3-carboxy-2- or 3-hydroxy-1-oxopropyl)-L-aspartic acid. This addition results in the terminal γ -linked glutamates being incorporated in the opposite orientation. In addition to these nonacylated MF coenzymes, we also identified the corresponding *N*-formyl-MF and, surprisingly, *N*-acetyl-MF derivatives. *N*-Acetyl-MF has never been observed or implied to be functioning in nature and may represent a new route for acetate formation in methanogens.



Methanofuran [MF (Figure 1)] is a coenzyme required for the first step of methanogenesis from CO_2 ,^{1–3} where it serves as a C1 carrier at the carbamate and formyl level of carbon oxidation in initial CO_2 reduction to formate.^{3,4} MF is also believed to be involved in the reverse chemical process for formaldehyde oxidation and detoxification in some archaea and bacteria.^{5,6} The first characterized structure of MF, designated here as MF-a, was of that from *Methanothermobacter thermoautotrophicus* (formerly *Methanobacterium thermoautotrophicum* strain ΔH).² *N*-Formyl-MF-a was shown to serve as an intermediate for the generation of methane in a wide range of methanogens, suggesting that the structure of MF was likely to be the same in all methanogens.⁷ However, subsequent structural characterization of MF coenzymes isolated from various methanogens demonstrated significant variation, and two new structures were described from *Methanosaicina barkeri*⁸ and *Methanobrevibacter smithii*,⁹ which are designated as MF-b and MF-c, respectively (Figure 1). Each MF contains a core structure of 4-[N -(γ -L-glutamyl- γ -L-glutamyl)- p -(β -aminoethyl)phenoxyethyl]-2-(aminomethyl)furan (APMF- γ -Glu₂) and differs on the basis of the composition of the attached side chain. MF-a contains 4,5-dicarboxyoctanedioic acid (DCO; also called 1,3,4,6-hexanetetracarboxylic acid) linked to the terminal glutamate residue, and MF-c contains hydroxyDCO in the same position. MF-b does not contain the DCO moiety but instead has four γ -linked glutamates.

Here we use liquid chromatography coupled with high-resolution mass spectrometry followed by traditional biochemical methods

to characterize two new MF structures in four different methanogens belonging to the order Methanococcales. MFs from organisms of this order have not been fully characterized until now. The MF present in the hyperthermophilic *Methanocaldococcus jannaschii* [MF-d (Figure 1)] is similar to MF-b, but it contains a longer γ -glutamyl tail with a range of 7–12 glutamates. The MF present in the mesophilic methanogens, *Methanococcus maripaludis* and *Methanococcus vannielii*, as well as the thermophilic *Methanothermococcus okinawensis* contains an unusual spacer in the side chain that we have identified as *N*-(3-carboxy-2-hydroxy-1-oxopropyl)-L-aspartic acid or *N*-(3-carboxy-3-hydroxy-1-oxopropyl)-L-aspartic acid [MF-e (Figure 1)]. In addition to the expected *N*-formylated derivatives, we also identified *N*-acetylated MF derivatives. This modification on MF has never been reported and may indicate a new route for the biosynthesis of an acetyl group.

MATERIALS AND METHODS

Chemicals. All chemicals and reagents were obtained from Sigma-Aldrich. Rat plasma was a gift from D. Ruggio (Department of Biochemistry, Virginia Polytechnic Institute and State University). 5-(Aminomethyl)-3-furanmethanol (F1) diacetate was synthesized as described previously.¹⁰

Received: August 5, 2014

Revised: September 4, 2014

Published: September 9, 2014



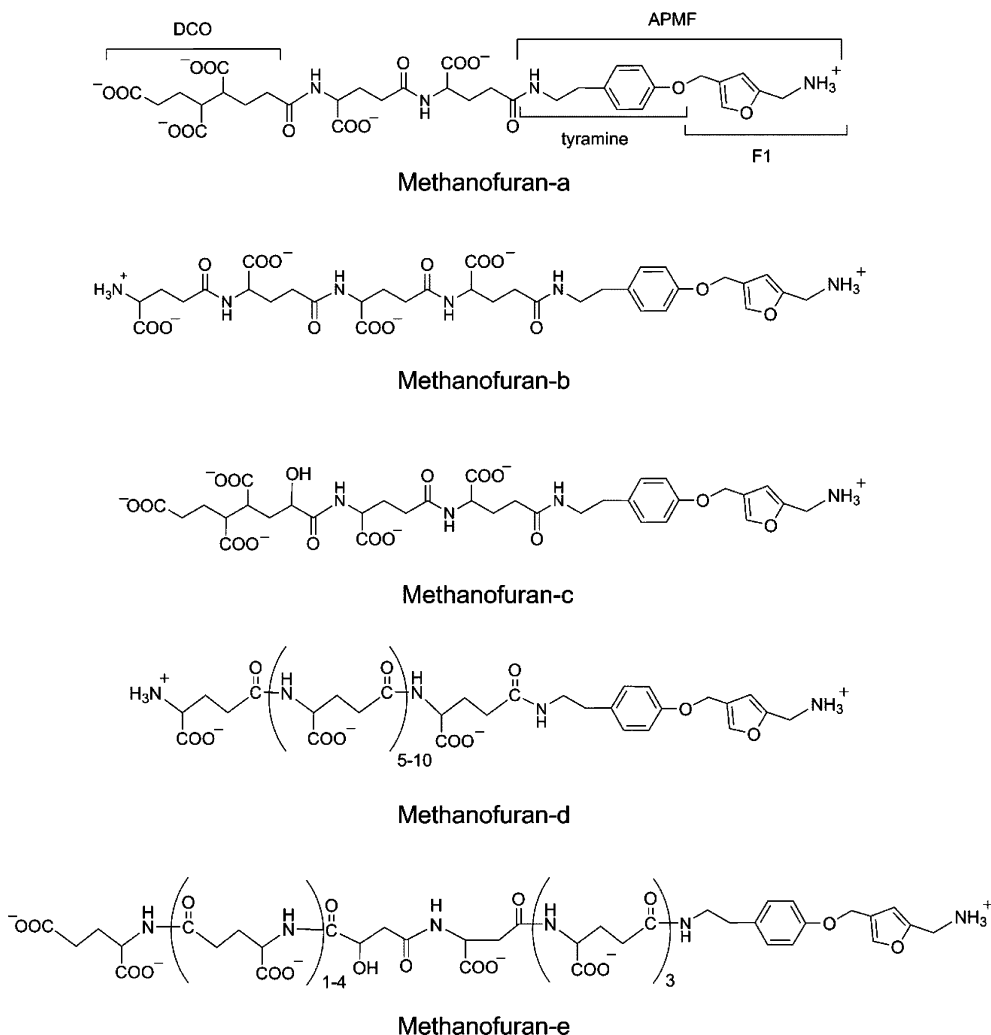


Figure 1. Chemical structures of currently characterized methanofurans. Methanofuran-d and methanofuran-e are described in this work.

Synthesis of Side Chain Components. *N*-(1,2-Dicarboxyethyl)-L-aspartic acid (Figure 9, III) was prepared by the reaction of maleic anhydride with L-aspartic acid. The reaction product was identified by gas chromatography–mass spectrometry (GC–MS) analysis of the trifluoroacetyl methyl (TM) derivative, where three separate peaks having $M^+ = 401$ were observed for the three different diastereomers. Fragment ions confirming $M^+ = 401$ were observed at $M^+ - 32 = 369$, $M^+ - 32 - 31 = 338$, $M^+ - 32 - 59 = 310$, and $M^+ - 59 - 32 - 32 = 278$. *N*-(Carboxymethyl)-L-glutamic acid (Figure 9, V) was prepared by reaction of glutamate in base with iodoacetate. The product produced a single peak on GC–MS analysis as the TM derivative showing $M^+ = 343$ with fragment ions at $M^+ - 32 = 311$, $M^+ - 59 = 284$, and $M^+ - 59 - 32 = 252$ with a base peak at 156.

Source of Methanogens. *M. jannaschii* JAL-1 was grown on a medium of inorganic salts as described previously.¹¹ *Mc. maripaludis* S2 and *Mt. okinawensis* were supplied by W. B. Whitman and were grown on McNA mineral medium containing 10 mM sodium acetate and 2% casamino acids as previously described.¹² *Mc. vannielii* was grown on a medium of defined salts containing formate and was supplied by T. C. Stadtman.¹³

Preparation of Cell Extracts. Frozen cell pellets (1 g) of each methanogen were added to a screw-capped test tube and suspended in 5 mL of water. To this suspension was added

6 mL of methanol, and the sample was sealed and heated while being shaken for 5 min at 100 °C. After being cooled, the samples were centrifuged and the pellets re-extracted in the same manner. The resulting extracts were combined and evaporated to ~0.5 mL with a stream of nitrogen. Large molecules were removed from the sample by being passed through an Amicon Ultra 3K centrifugal filter (Millipore). The final sample was concentrated to 0.15 mL for analysis.

Liquid Chromatography–High-Resolution Mass Spectrometry (LC–HR-MS) Analysis of Cell Extracts. The cell extracts were then analyzed directly on a Waters SYNAPT G2-S high-definition mass spectrometer connected to a Waters Acquity UPLC I-class system with an Acquity UPLC BEH C18 (Waters, 2.1 mm × 75 mm, 1.7 μm particle size) column. Solvent A was water with 0.1% formic acid, and solvent B was acetonitrile. The flow rate was 0.2 mL/min, and gradient elution was conducted in the following manner (t (minutes), % B): (0.01, 5), (6, 15), (21, 35), (23, 65). Ten microliters of the sample was injected. The mass spectral data were collected in high-resolution MSe continuum mode. A lock spray scan (Function 3) was collected every 20 s for calibration, and the lock spray analyte used was Leucine-Enkephalin. The parameters were as follows: 2.8 kV capillary voltage, 125 °C source temperature, 350 °C desolvation temperature, 35 V sampling cone, 50 L/h cone gas flow, 500 L/h desolvation gas flow, and

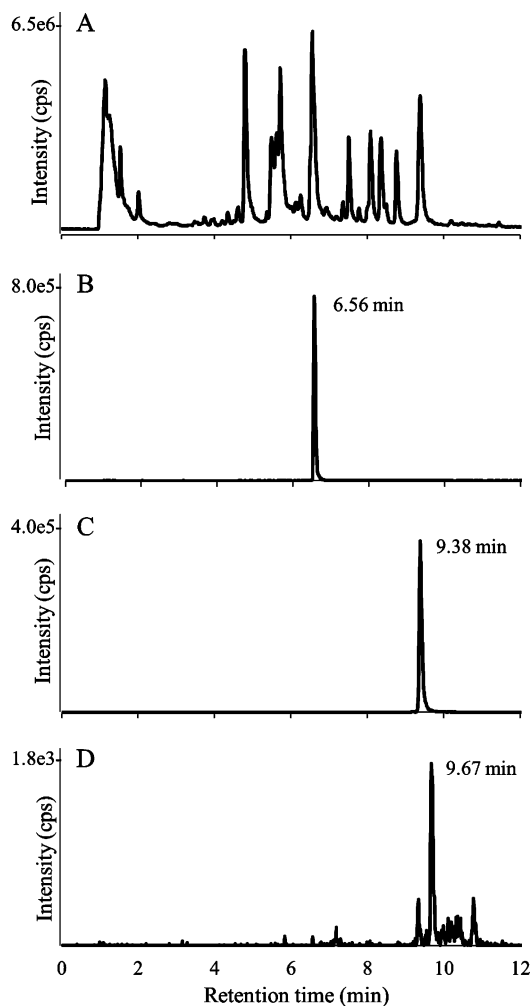


Figure 2. LC–HR-MS analysis of the *M. jannaschii* cell extract: (A) TIC chromatogram, (B) 769.2884 extracted ion current (XIC) chromatogram corresponding to the MH_2^{2+} for MF-d-10, (C) 783.2877 XIC chromatogram corresponding to the MH_2^{2+} for formyl-MF-d-10, and (D) 790.2979 XIC chromatogram corresponding to the MH_2^{2+} for acetyl-MF-d-10.

6 L/h nebulizer gas flow. The collision energies for the low-energy scans (Function 1) were 4 and 2 V in the trap region and transfer region, respectively. Collision energies for the high-energy scans (Function 2) were ramped from 25 to 45 V in the trap region and 2 V in the transfer region.

Isolation of Methanofuran from Cell Extracts. A portion of the cell extract was further purified by chromatographic separation performed on a Shimadzu Prominence UFLC system equipped with a photodiode array detector (PDA) and a fluorescence detector. A strong anion exchange column (Shodex QA-825, 8.0 mm × 75 mm, 12 μm particle size) was used at a flow rate of 1 mL/min, and the elution profile consisted of a 5 min water wash followed by a 40 min linear gradient to 2 M ammonium bicarbonate. A 0.1 mL volume was injected, and 1 mL fractions were collected. The fractions containing MF were combined, and the ammonium bicarbonate was removed with a stream of nitrogen gas while the samples were heated at 100 °C. The sample was resuspended in 0.1 mL of water for further analysis.

Liquid Chromatography–Ultraviolet–Visible Spectrophotometry–Mass Spectrometry (LC–UV–MS) Analysis. To simultaneously obtain the absorbance spectra and mass

Table 1. Measured Doubly and Singly Charged Positive Ions with the Calculated Molecular Mass for the Methanofuran Present in *M. jannaschii* (MJ), *Mc. maripaludis* (MM), *Mc. vannielii* (MV), and *Mt. okinawensis* (MO)

peak name (retention time)	MH_2^{2+}	MH^+	calculated mass from MH_2^{2+} and MH^+
MJ MF-d-10 (6.56 min)	769.2884	1537.5679	1536.5601 1536.5601
MJ formyl-MF-d-10 (9.38 min)	783.2877	1565.5686	1564.5571 1564.5571
MJ acetyl-MF-d-10 (9.67 min)	790.2979	ND	1578.5802 1578.5802
MM MF-e-7+ (5.30 min)	691.2432	1381.4824	1380.4746 1380.4704
MM formyl-MF-e-7+ (7.95 min)	705.2415	1409.4752	1408.4674 1408.4674
MM acetyl-MF-e-7+ (8.23 min)	712.2496	1423.4917	1422.4836 1422.4839
MV MF-e-7+ (5.32 min)	691.2432	1381.4824	1380.4708 1380.4746
MV formyl-MF-e-7+ (7.95 min)	ND	ND	1408.4674 ^a 1408.4674 ^a
MV acetyl-MF-e-7+ (8.24 min)	712.2496	1423.4917	1422.4836 1422.4839
MO MF-e-7+ (5.31 min)	691.2432	1381.4824	1380.4836 1380.4836
MO formyl-MF-e-7+	ND	ND	N/A
MO acetyl-MF-e-7+	ND	ND	N/A

^aCalculated from the ions observed in negative mode: $(\text{M} - 2\text{H})^{2-} = 703.2321$ and $(\text{M} - \text{H})^- = 1407.4625$. ND denotes not detected.

spectral data of the MF derivatives, analyses were also performed using an Agilent 1200 Series liquid chromatograph with a Zorbax Eclipse XDB-C18 column (Agilent, 4.6 mm × 50 mm, 1.8 μm particle size) equipped with a PDA detector interfaced with an AB Sciex 3200 Q TRAP ESI mass spectrometer. Solvent A was water with 0.1% formic acid, and solvent B was methanol with 0.1% formic acid. The flow rate was 0.5 mL/min, and gradient elution was employed in the following manner (*t* (minutes), % B): (0.01, 5), (10, 65), (15, 65). Ten microliters of the sample from anion exchange purification was injected. The mass spectral data were collected in positive mode, and electrospray ionization was employed at 4500 V and 400 °C. The curtain gas was set at 35 au, and GS1 and GS2 were 60 and 50 au, respectively. Analyst software (Applied Biosystems/MDS SCIEX) was used for system operation and data processing.

Analysis of 5-(Aminomethyl)-3-furanmethanol (F1) from MF-d and MF-e. The ion exchange-purified fractions containing MF-d and MF-e were subjected to hydrolysis with 1 M HCl for 5 min at 100 °C, and after evaporation of the acid, the released F1 was purified by preparative TLC. The purified F1 was converted to its 4-fluoro-7-nitrobenzofurazan (NBD-F)

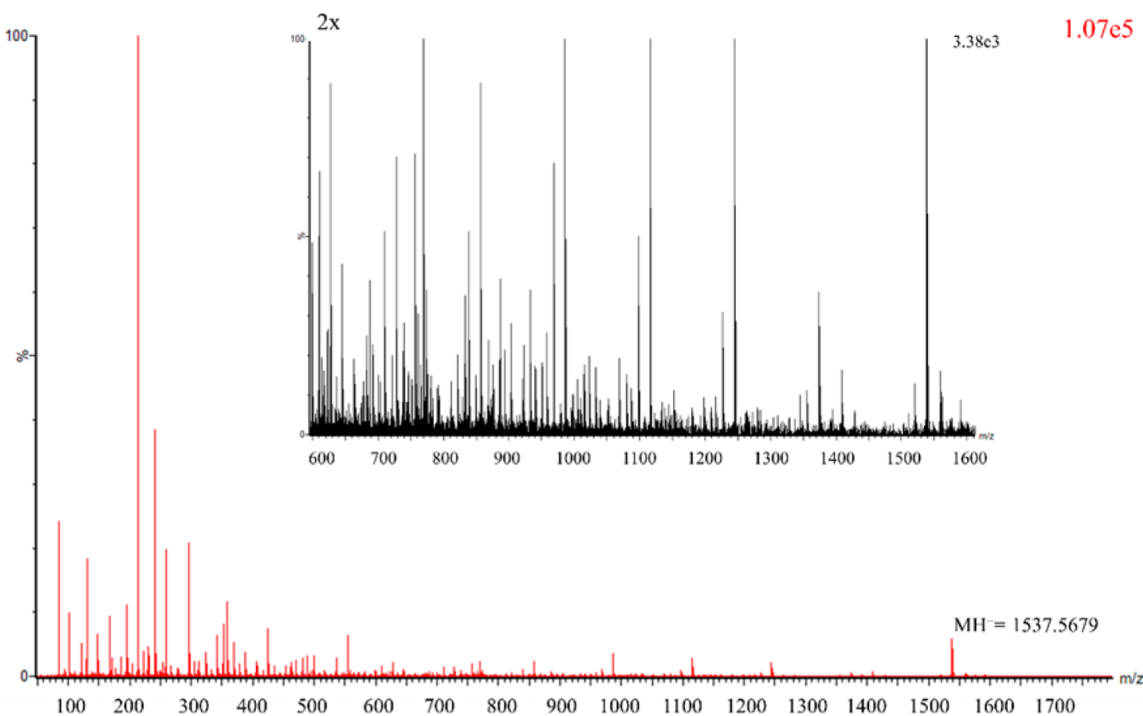


Figure 3. High-energy CID mass spectrum of MF-d-10. The inset is an expanded and magnified (2 \times) version of the spectrum to highlight the fragmentation pattern.

derivative as recently¹⁴ and analyzed by HPLC with fluorescence detection and LC–UV–MS to confirm the presence of the expected F1 in purified MF-d and MF-e.

Analysis of the MF-d Side Chain. Fractions from the anion exchange purification containing MF-d were evaporated to dryness, dissolved in 0.5 mL of 6 M HCl, and heated at 110 °C 24 h followed by GC–MS analysis of the TM derivatives of the resulting compounds. Glutamate present from the acid hydrolysis was reacted with 1-fluoro-2,4-dinitrophenyl-5-L-alanine amide (FDAA) to form the diastereomeric derivative and then analyzed by HPLC as previously described.¹⁵

The anion exchange-purified MF-d samples were treated with peptidases specific to either α - or γ -linked amino acids. Enzymatic reaction conditions consistent with the manufacturer's recommendations were used. Endoproteinase Glu-C from *Staphylococcus aureus* V8, which specifically cleaves peptide bonds on the carboxyl side of α -bound L-aspartate and L-glutamate, resulted in no change in the molecular weight of MF-d or the appearance of a new product as determined by matrix-assisted laser desorption ionization (MALDI) MS analysis. Likewise, treatment of MF-d with rat plasma containing γ -glutamyl hydrolase¹⁶ resulted in no change in the molecular weight of the product or the appearance of a new product, as determined by MALDI MS analysis. As positive controls for enzyme activity, Glu-C and γ -glutamyl hydrolase were shown to be active with peptides containing α -linked L-glutamates and folate-containing γ -linked L-glutamates, respectively.

Analysis of the MF-e Side Chain. Fractions from the anion exchange purification containing MF-e were evaporated to dryness, dissolved in 0.5 mL of 6 M HCl, and heated at 110 °C for 24 h. After evaporation of the acid, the samples were dissolved in 200 μ L of water and applied to a Dowex 50W-8X-H⁺ column (0.5 cm \times 2 cm) and eluted with 1 mL fractions of

water, 0.1 M HCl, and 0.5 M HCl. The malic acid was present only in the water fraction, and the aspartic acid and glutamic acid were in both the 0.1 M HCl and 0.5 M HCl fractions. The acid was evaporated, and the TM derivatives were formed by heating the sample in 3M HCl in methanol followed with a 1:1 mixture of trifluoroacetic anhydride and methylene chloride. The samples were then carefully evaporated at room temperature and dissolved in methyl acetate for GC–MS analysis. This is a critical step in the procedure due to the ready evaporation of the malic acid derivative during concentration of the sample. Quantitation of malate compared to the other compounds present in MF-e was not possible with this method because the TM derivative was so volatile that even minimal sample processing interfered with recovery.

To determine if the MF-e contained an ester linkage in the spacer molecule, we dissolved a sample of anion exchange-purified MF-e in 6 M ammonium hydroxide for 30 min at room temperature. After evaporation, the sample was examined by MALDI MS to determine if ammonia lysis had occurred. No indication of cleavage was seen; therefore, the MF-e does not contain an ester linkage that would be susceptible to base hydrolysis.

Gas Chromatography–Mass Spectrometry (GC–MS) Analyses. GC–MS analysis of hydrolysis products was conducted using a VG-70-70EHF mass spectrometer operating at 70 eV and equipped with an HP-5 column (0.32 mm \times 30 m) programmed from 95 to 280 °C at a rate of 10 °C/min. Under the GC–MS conditions employed, the TM derivatives of the following compounds had the following retention times (seconds) and mass spectral data (molecular weight, base peak, and the most abundant ions with masses of m/z > 50 listed in order of decreasing intensity): malic acid TM derivative (273 s) (258, 59, 113, 117, 69, 85, 157, 227), aspartic acid TM derivative (406 s) (257, 198, 156, 166, 59, 69, 85, 113, 226, 225), glutamic acid TM derivative (537 s) (271, 152, 212, 180,

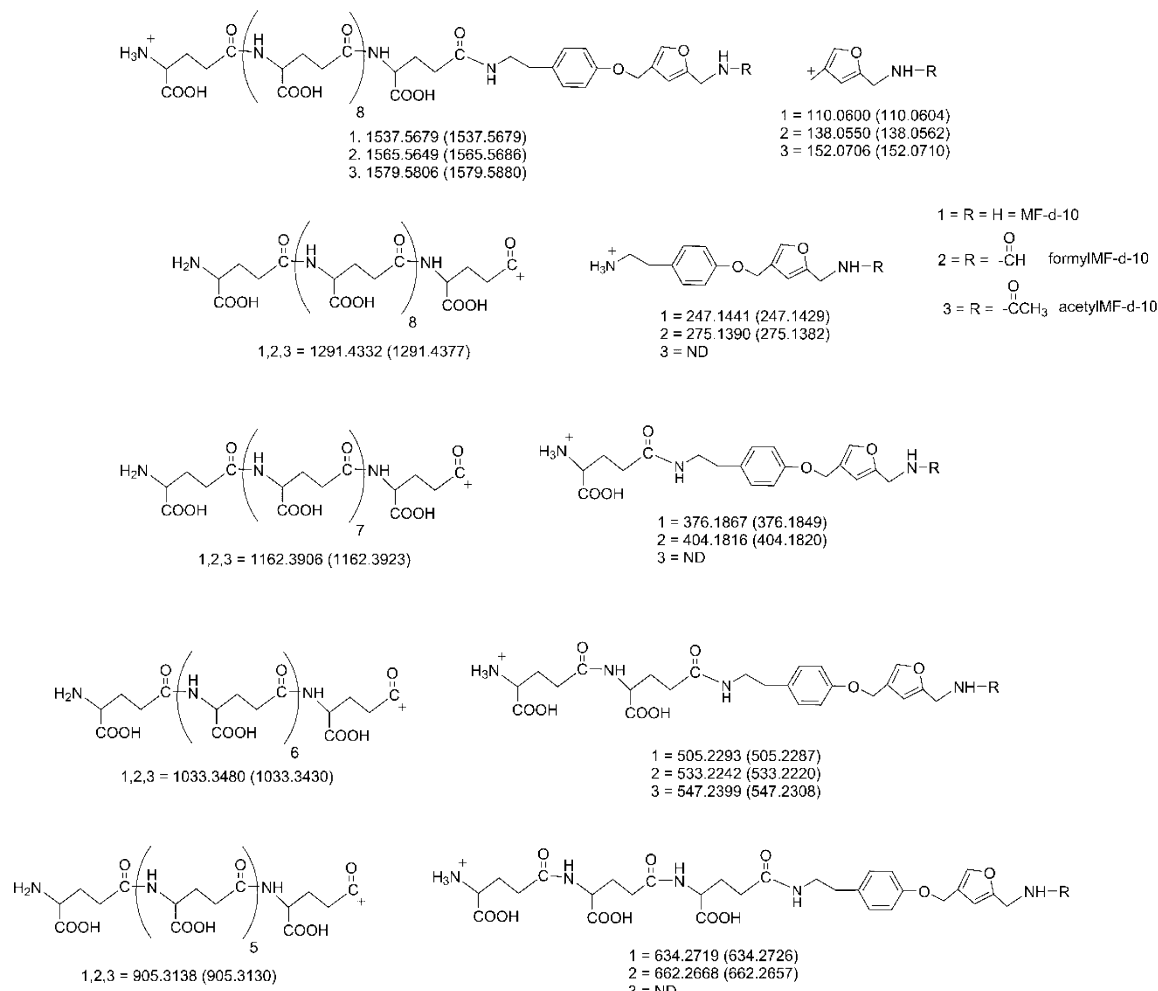


Figure 4. Calculated masses (observed masses) and proposed structures of the fragments supporting the structure of MF-d-10 from *M. jannaschii*. The masses reported were measured from MF-d-10, but similar fragments were obtained from the other MF-d molecules with varying numbers of glutamates. The positions of the positive charges are only proposed. ND denotes not detected.

69, 59, 85, 94, 239, 240). The tyramine as the difluoroacetyl derivative was observed at (454 s) (329, 216, 126, 119, 175, 109).

NMR Analysis. Anion exchange-purified MF-d fractions were evaporated to dryness using a stream of nitrogen gas at 100 °C to remove the ammonium bicarbonate, and the sample was dissolved in D₂O for NMR analysis. ¹H NMR data were collected on a Varian Inova 400 MHz instrument at the Virginia Polytechnic Institute and State University NMR spectroscopy center.

RESULTS

High-Resolution Mass Spectral Analysis of *M. jannaschii* Extracts. As part of an effort to discover and characterize previously unrecognized metabolites in methanogens, we analyzed *M. jannaschii* cell extracts by LC–HR-MS. At least 10 major peaks were observed on the basis of the total ion current (TIC) chromatographic trace (Figure 2). The trace recorded under high-energy collision-induced dissociation (CID) conditions used to induce fragmentation looked analogous (not shown). Analysis of the mass spectral data indicated that none of the known MF structures were present in *M. jannaschii*. Instead, two of the largest peaks observed at 6.56 and 9.38 min caught our attention, and data obtained from these peaks will be considered here. Many of the remaining

peaks corresponded to other methanogenic cofactors such as coenzyme F₄₂₀, coenzyme F₄₃₀, and methanopterin derivatives. In the low-energy mass spectrum of the compound eluting at 6.56 min, the most intense ion had an $\text{MH}_2^{2+} = 769.2884$ corresponding to a monoisotopic molecular mass of 1536.5601 (Table 1). The major compound in the 9.38 min peak showed an $\text{MH}_2^{2+} = 783.2877$ corresponding to a monoisotopic molecular mass of 1564.5571 (Table 1). The difference between these masses is 27.997 (calculated mass for CO of 27.995) and indicated that the second peak was a formamide derivative of the first. A minor compound eluting at 9.67 min (Figure 2) showed an $\text{MH}_2^{2+} = 790.2927$ corresponding to a monoisotopic mass of 1578.5802 (Table 1). The difference between these masses and the mass of the compound in the 6.56 min peak, 42.0128 and 42.0093, respectively, represents the addition of C₂H₂O (calculated mass of 42.0106) and indicates that the compound at 9.67 min is an acetyl derivative. The sodiated ions with the correct masses were additionally observed for these molecules. In negative ion mode, ($\text{M} - 2\text{H}$)²⁻ and ($\text{M} - \text{H}$)⁻ ions were observed with the expected exact masses.

When this sample was analyzed in high-CID mode, the doubly charged ions disappeared and abundant fragment ions and MH^+ ions were observed (Figure 3). Many of the fragment ions were separated by 129.0425, corresponding to the presence of several glutamates in the molecules. In addition,

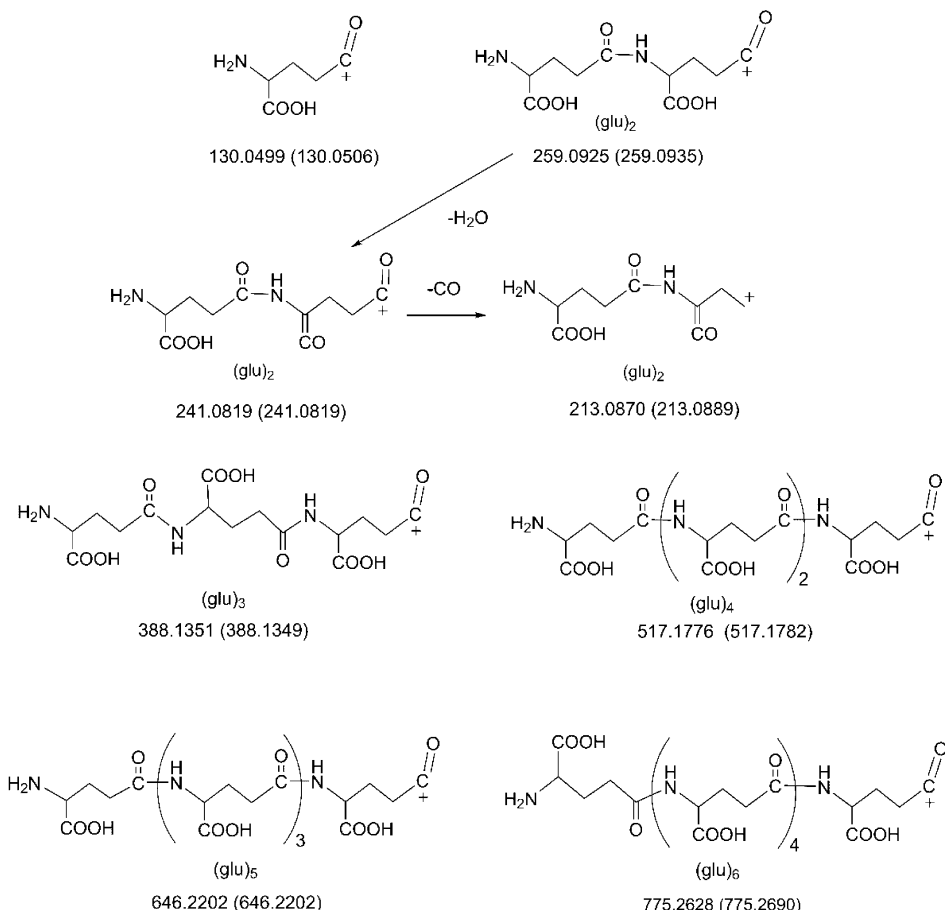


Figure 5. Calculated masses (observed masses) and proposed structures for glutamate-related fragments commonly observed for all MF compounds reported here. All of these fragments additionally showed intense multiple H_2O losses.

centered on either side of the elution position of the major compounds in each peak were a series of additional molecules that differed by 129.0425, indicating the presence of compounds with the same core structure and separated by the number of glutamates present. These various glutamate homologues differed in retention times by ~ 0.1 min, with molecules containing more glutamates eluting after molecules containing fewer glutamates.

These observations, in addition to the experiments described below, are consistent with the major compounds in the 6.56 min peak being MF with 7–12 glutamates in the side chain. We have designated this molecule as MF-d to indicate that it is the fourth MF to be structurally characterized (Figure 1). The second peak at 9.38 min contains formyl-MF-d with 7–12 glutamates in the side chain, and the compound eluting at 9.67 min is acetyl-MF-d (Figure 2). The relative levels of MF-d-7, MF-d-8, MF-d-9, MF-d-10, MF-d-11, and MF-d-12 (the number indicates the total number of glutamates present) were 2.1, 3.2, 29, 100, 28, and 3.4, respectively. The formyl-MF-d had a similar polyglutamate distribution, indicating that each of the MF-d coenzymes with varying numbers of glutamates is being biochemically carbamated and reduced to the formylated MF by formyl-methanofuran dehydrogenase to the same extent. The approximate ratio of the total amount of MF-d and formyl-MF-d based on the intensities of their MH^+ ions was 1:1. Acetyl-MF-d-10 was the only acetyl-MF-d derivative detected, likely because the levels of homologues with differing numbers of glutamates were too low to accurately

measure. On the basis of the measured MH_2^{2+} ion intensities, the amount of acetyl-MF-d-10 represented 0.36% of the MF-d-10 in *M. jannaschii*.

Figure 4 shows the proposed complete structures of MF-d-10 and some of the observed structurally important fragments along with their calculated and observed masses. The observed fragmentation supports a structure in which the side chain attached to the tyramine consists exclusively of γ -linked glutamates. The most intense fragments observed containing the nonacylated, formylated, and acetylated furan had expected masses of 110.0604, 138.0562, and 152.0710, respectively (Figure 4). These cationic species are reminiscent of the benzyl cation seen via electron impact mass spectrometry, which is well-known for its stability. The mass differences are consistent with the addition of a formate and an acetate to the amino group of the furan and demonstrate that only this change is responsible for the different masses observed for the intact molecules.

Figure 5 shows the proposed structures and the calculated and measured masses of the smaller glutamate-derived fragments observed to be common to all the structures reported here. The measured masses further support the presence of linearly γ -linked glutamates that are attached to the tyramine portion of $[(\beta\text{-aminoethyl})\text{phenoxy}]\text{-}2\text{-(aminomethyl)furan}$ (APMF) (Figure 1).

Chemical and Biochemical Characterization of MF-d from *M. jannaschii*. To support the high-resolution mass spectrally derived structures, MF-d was isolated from the cell

extraction mixture by anion exchange chromatography for further characterization. Because of the strong anionic nature of these compounds, all MF-d molecules eluted in the same fraction. Analysis of the fraction by HPLC interfaced with a photodiode array detector and a mass spectrometer (LC–UV–MS) showed two peaks with the first containing MF-d-7–12 and the second containing the formyl-MF-d-7–12 based on the detection of their respective MH_2^{2+} ions. Each peak had UV absorbance maxima at 215 and 274 nm, the same reported for previously characterized MF-a.^{2,3} On the basis of the absorbance data, the abundance of MF-d and formyl-MF-d was 1:1. This ratio agrees with the mass spectral data, indicating that both molecules ionize to the same extent.

¹H NMR analysis of the purified sample of MF-d and formyl-MF-d showed resonances at δ_{H} 6.55 (1H, s) and δ_{H} 7.60 (1H, s) and at δ_{H} 7.05 (2H, d) and δ_{H} 7.30 (2H, d), confirming the presence of the furan and tyramine, respectively.^{2,3,8} The formyl proton of formyl-MF-d was also observed at δ_{H} 8.12 (1H, s). Broad resonances centered at δ_{H} 4.10, 2.06, and 2.40 for the α , β , and γ protons, respectively, of the polyglutamates were observed, consistent with the data reported previously for MF-b.⁸

Acid hydrolysis of the isolated MF-d followed by GC–MS analysis of the TM derivatives of the resulting compounds confirmed the presence of glutamate and tyramine. The L-configuration of glutamate was demonstrated by HPLC analysis of the diastereomeric FDAA derivative and confirmed that only L-glutamate is present in MF-d. Acid hydrolysis of another portion of the mixture produced F1, a known hydrolysis fragment of MF (Figure 1)^{2,9} that was analyzed by LC–UV–MS as its NBD derivative.¹⁴

To provide evidence that the glutamates in the side chain were γ -linked rather than α -linked, we treated the purified MF-d with hydrolytic peptidases known to hydrolyze both α -linked endo- and exoglutamate. These enzymes failed to alter any of the MF-d molecules, as evidenced by MALDI mass spectral analysis. We also treated the MF-d with rat plasma conjugase, which removes terminal γ -linked L-glutamates¹⁶ as found in folate. This enzyme was also unable to hydrolyze the glutamate linkages in MF-d. These data are consistent with all the molecules containing only γ -linked L-glutamates with the γ -carboxy terminal of the polyglutamates being bound to the amino group of the tyramine as seen in MF-b (Figure 1). This type of linkage results in a free amino and carboxy on the side chain terminus (Figure 1) rather than just the carboxy terminus found in folate γ -polyglutamates.

Analysis of *Mc. maripaludis* Cell Extracts. LC–HR-MS analysis of *Mc. maripaludis* cell extracts under low-energy conditions produced the TIC trace shown in Figure 6. As observed with the *M. jannaschii* cell extract, the trace recorded under high-energy conditions looked similar. Analysis of the mass spectral data indicated that none of the previously described MF coenzymes or the MF-d molecules found in *M. jannaschii* were present in *Mc. maripaludis*. Peaks at 5.30, 7.95, and 8.23 min were proposed to contain MF-e, formyl-MF-e, and acetyl-MF-e, respectively, on the basis of their mass differences (Table 1). The large difference in retention time compared to that of *M. jannaschii* MF-d is due to different LC conditions and not necessarily to structural differences. We have designated this new MF structure as MF-e to indicate that it is the fifth methanofuran to be structurally characterized. After accounting for the mass of one glutamate residue (129.0426), we found the difference between the

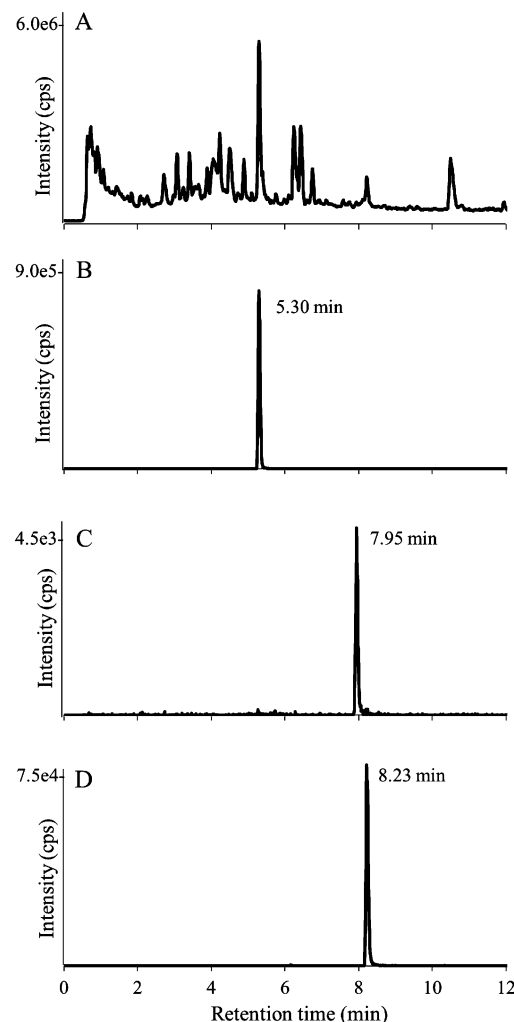


Figure 6. LC–HR-MS analysis of the *Mc. maripaludis* cell extract: (A) TIC chromatogram, (B) 691.2432 extracted ion current (XIC) chromatogram corresponding to the MH^{2+} for MF-e-7+, (C) 705.2415 XIC chromatogram corresponding to the MH^{2+} for formyl-MF-e-7+, and (D) 712.2496 XIC chromatogram corresponding to the MH^{2+} for acetyl-MF-e-7+.

masses of the major compounds in these peaks and the corresponding peaks in *M. jannaschii* was 27.0488.

Adjacent to each of these peaks were corresponding homologues containing different numbers of glutamate residues, with each of these accounting for less than 10% of the major central peak. MF-e-5+ [contains five glutamate residues plus (+) an additional piece], MF-e-6+, MF-e-7+, MF-e-8+, and MF-e-9+ were present at relative ratios of 0.47, 1.5, 100, 1.4, and 0.44, respectively. Only formyl-MF-e-7+ and formyl-MF-e-8+ were detected, with formyl-MF-e-8+ representing only 4% of the formyl-MF-e-7+ peak. Similarly, only acetyl-MF-e-7+ and acetyl-MF-e-8+ were detected, with acetyl-MF-e-8+ being only 4% of the acetyl-MF-e-7+ peak. This result indicates that MF-e-7+ is the predominant MF coenzyme in these cells, and the distribution of the polyglutamates is less varied compared to that of MF-d in *M. jannaschii*. Formyl-MF-e and acetyl-MF-e represented 0.5 and 8%, respectively, of the total MF-e present in *Mc. maripaludis*.

Our following results will focus only on the major peak in each group, MF-e-7+. In the low-energy mass spectrum, the major ions observed were the MH_2^{2+} as well as the MH^+ ions.

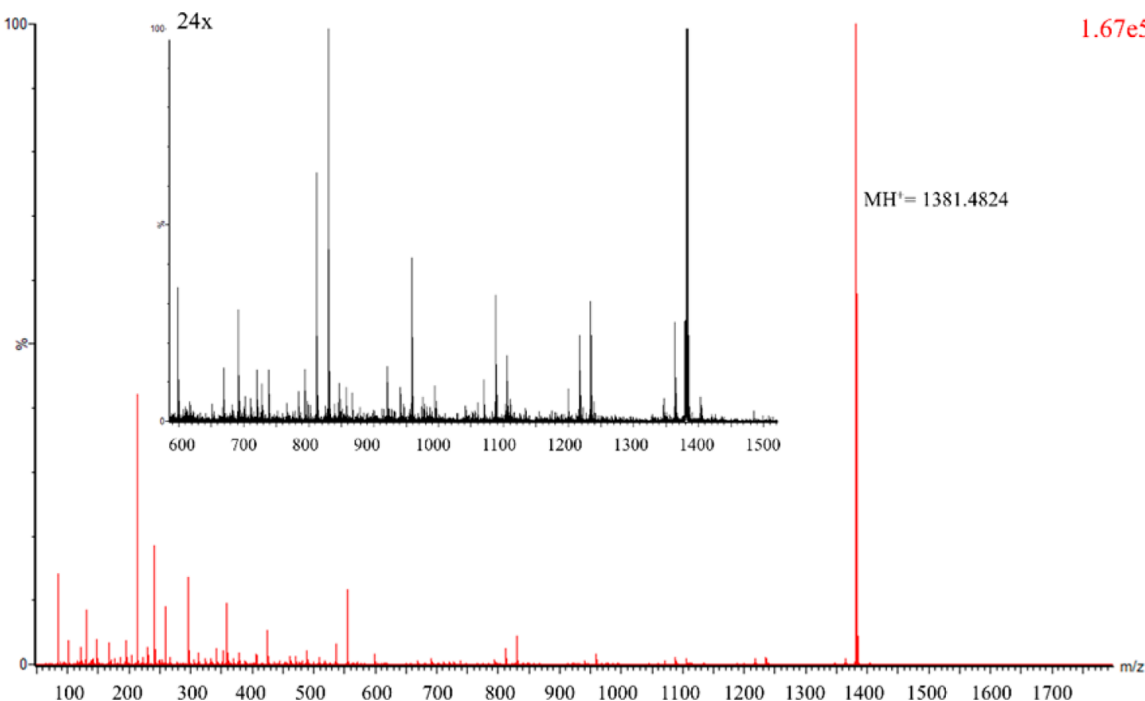


Figure 7. High-energy CID mass spectrum of MF-e-7+. The inset is an expanded and magnified (24×) version of the spectrum to highlight the fragmentation pattern.

In the high-energy spectra, the MH_2^{2+} ion was not observed but MH^+ was more intense, and some informative fragment ions were observed (Figure 7). The observed masses for the MH_2^{2+} and MH^+ ions are listed in Table 1. The major compound in the peak at 5.30 min had an $\text{MH}_2^{2+} = 691.2432$ and $\text{MH}^+ = 1381.4824$, corresponding to a monoisotopic mass of 1380.4724 (average). The major compound in the second peak at 7.95 min with an $\text{MH}_2^{2+} = 705.2415$ and $\text{MH}^+ = 1409.4752$ corresponded to a monoisotopic mass of 1408.4674. The difference between these masses indicated the second peak was the formamide derivative of the compound in the peak at 5.30 min. The major compound in the third peak at 8.22 min with an $\text{MH}_2^{2+} = 712.2496$ and $\text{MH}^+ = 1423.4917$ corresponded to a monoisotopic mass of 1422.4837, indicating the addition of an acetate. Masses of $(\text{M} - 2\text{H})^{2-}$ and $(\text{M} - \text{H})^-$ were also observed with the expected exact masses.

Chemical Characterization of MF-e from *Mc. maripaludis*. Although the results for the MF-e present in *Mc. maripaludis* were similar to the observations in *M. jannaschii*, the masses of the parent ion and many of the fragment ions did not match, even after correcting for differing numbers of glutamates, indicating that there were fundamental differences in the MF structure in these two methanogens. Significantly, the MF-e did not fragment as readily as we observed for MF-d under the same conditions (Figures 3 and 7). The fragment ions from the furan terminus of MF-e were all identical to those observed with MF-d up to the fragments containing three glutamates (Figure 4). These ions were 27.9924 higher for the formyl-MF and 42.0093 higher for the acetyl-MF. The fragments resulting from the loss of side chain terminal glutamates were different from those detected in *M. jannaschii* extracts in that they contained a MH^+ glutamate = 148.0610 (glutamate residue mass + $\text{H}_2\text{O} + \text{H}^+$), indicating the presence of a terminal glutamate bound via its nitrogen as an amide linkage to the structure (Figure 1). This is the opposite orientation of the terminal glutamate present in the side chain

of MF-b and MF-d (Figure 1). Also observed were the MH^+ ions for $(\text{Glu})_2$, $(\text{Glu})_3$, and $(\text{Glu})_4$ (Figure 8). Clear losses of polyglutamates from the side chain terminus with charge retained on the furan portion of the molecule were observed up to the loss of four glutamate residues, at which point they ended (Figure 8). These observations indicated that a different component was present at this point in the structure. This component would have to change the orientation of the glutamates and have a residue mass of 215.0430 corresponding to $\text{C}_8\text{H}_9\text{NO}_6$. To change the glutamate orientation, two carboxylic acids in the compound would be required to bind as amides to two different glutamates in the structures.

To determine the identity of the unknown chemical moiety present in the MF-e side chain, we developed a list of possible compounds based on the criteria mentioned above and tested whether they matched the characteristics of the unknown. All the compounds shown in Figure 9 have the correct residue mass; however, only *N*-(3-carboxy-3-hydroxy-1-oxopropyl)-L-aspartic acid (**I**) or *N*-(3-carboxy-2-hydroxy-1-oxopropyl)-L-aspartic acid (**II**) fit with all the data we obtained. Both **I** and **II** represent an aspartate linked to a malate via an amide bond. Each has the correct residue mass, and each can change the orientation of the polyglutamates upon being inserted into the middle of the side chain. Most significantly, upon acid hydrolysis of MF-e, we observed malate and aspartate by GC-MS analysis, providing convincing evidence that either **I** or **II** is the unique spacer moiety present in MF-e. We currently have no way to determine the exact orientation of this molecule in the structure.

Further analyses were performed to rule out the other spacer possibilities. *N*-(Dicarboxymethyl)-L-glutamic acid (**IV**) would be decarboxylated during acid hydrolysis to produce *N*-(carboxymethyl)-L-glutamic acid (**V**). *N*-(1,2-Dicarboxyethyl)-L-aspartic acid (**III**) and **V** were each chemically synthesized, shown to be resistant to acid hydrolysis, converted to their TM derivatives, and analyzed by GC-MS. The data demonstrated

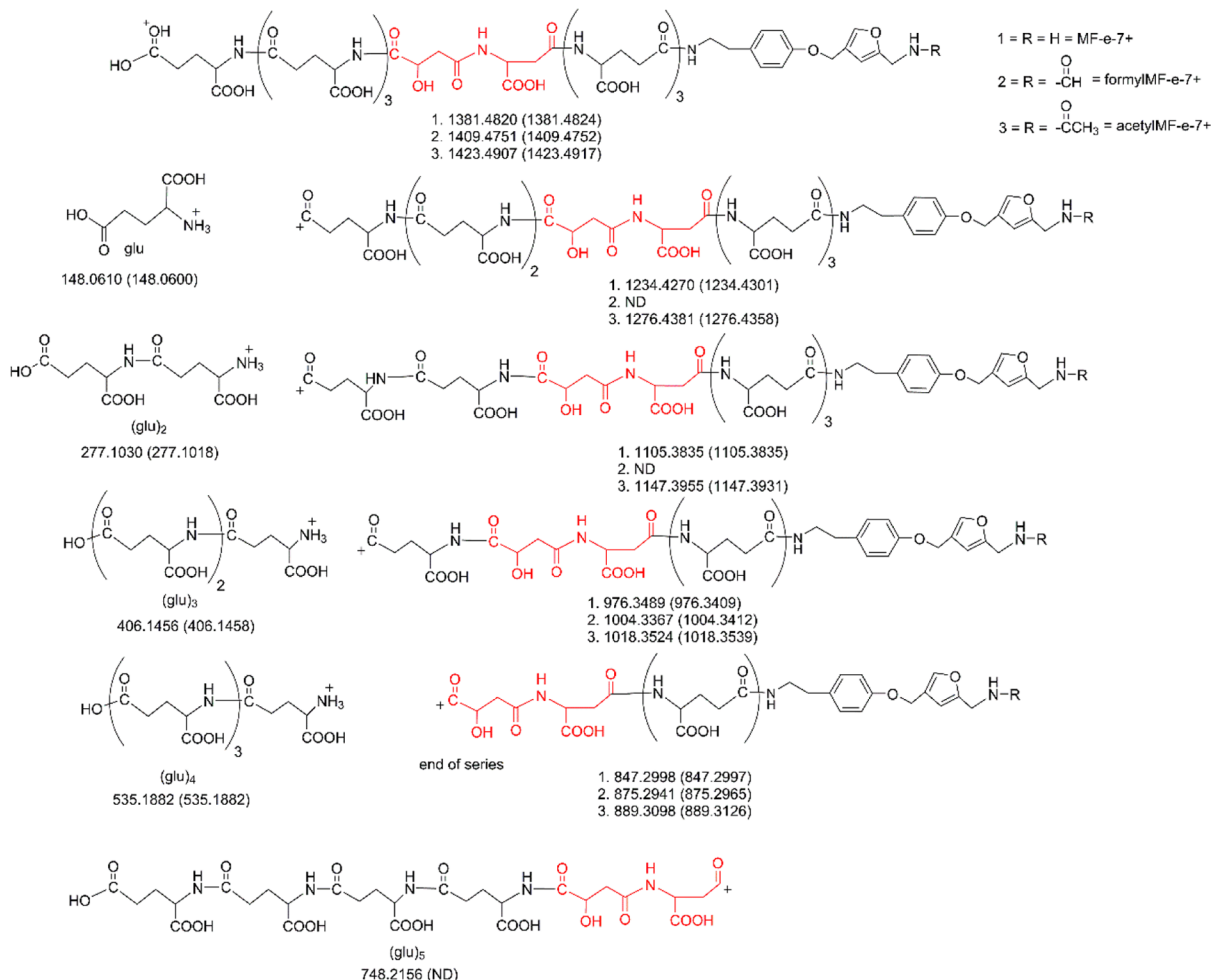


Figure 8. Calculated masses (observed masses) and proposed structures of MF-e-7+ and some of its structurally informative fragments. The red atoms represent the unique spacers present in the middle of the polyglutamate side chains, which likely consist of an aspartate and malate residue. ND denotes not detected.

that neither of these compounds was produced after acid hydrolysis of MF-e. On the basis of the predicted mass spectrum of the TM derivative of 2-amino-1,2,3,5-butanetetracarboxylic acid (**VI**), this compound was also not produced by the acid hydrolysis of MF-e. Compound **VII** was eliminated because it contained an ester linkage, which was shown to be absent in MF-e.

To confirm the identity of the acetylated furan, we examined a synthetic standard of F1-diacetate by LC-MS. As shown in Figure 10, the molecule undergoes the loss of acetic acid to form the indicated benzyl cation that then loses ketene to form the 110.0600 ion. These are the same ions seen upon fragmentation of the acetylated MF-e derivatives.

Analysis of *Mc. vannielii* Cell Extracts. The results for the analysis of the MF found in *Mc. vannielii* were very similar to those discussed above for *Mc. maripaludis*. The data for MF-e-7+ and acetyl-MF-e-7+ from both *Mc. maripaludis* and *Mc. vannielii* cells were identical in all respects, including retention times, measured masses, and fragment ion intensities. The one exception was that formyl-MF-e was not detected in *Mc. vannielii* extract, likely just because of its low abundance. MF-e-5+, MF-e-6+, and MF-e-7+ were detected with relative ratios of 1.0, 5.1, and 100, respectively. Acetyl-MF-e-5+, acetyl-MF-e-6+, and acetyl-MF-e-7+ were detected with relative ratios of 13.6, 43.2, and 100, respectively.

Acetyl-MF-e represented 16% of MF-e in *Mc. vannielii* on the basis of the measured intensities of the MH_2^{2+} ions.

Analysis of *Mt. okinawensis* Cell Extracts. *Mt. okinawensis* extracts also contained MF-e. MF-e-4+, MF-e-5+, MF-e-6+, MF-e-7+, and MF-e-8+ were detected with relative ratios of 1.3, 1.8, 5.3, 100, and 1.6, respectively. Neither formyl nor acetyl derivatives could be detected in these cells.

DISCUSSION

Importance of These Methanofurans. This is the first report describing the complete structures of the MFs present in archaea from the order Methanococcales. The two unique MF structures described here, MF-d and MF-e, contain the APMF core structure (Figure 1) as found in all currently known MF coenzymes.⁹ For MF-d and MF-e, this core structure is covalently bound to the γ -position of a γ -polyglutamate containing at least four glutamate residues. This is similar to MF-b found in *Msc. barkeri*, a mesophilic methylotrophic methanogen of the order Methanosaecinales. MF-a was identified in *Mtb. thermoautotrophicus*, a thermophilic hydrogenotrophic methanogen of the order Methanobacteriales, and MF-c was characterized from *Mbb. smithii*, a mesophile also of the order Methanobacteriales.

Comparison to Other Glutamate-Containing Coenzymes. The side chains of MF-d and MF-e contain poly γ -linked

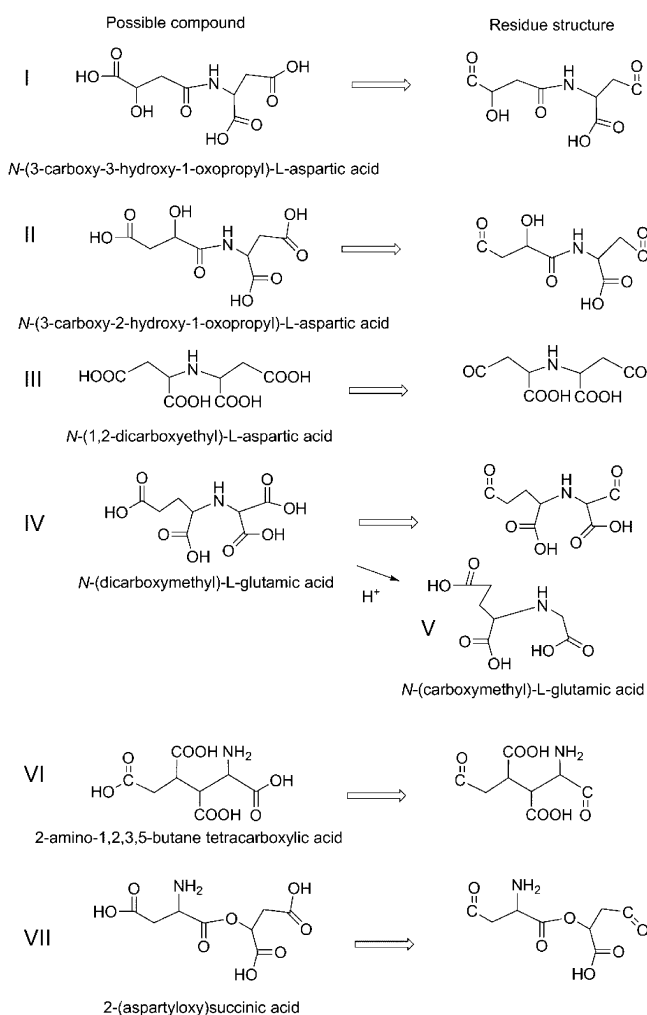


Figure 9. Possible MF-e side chain spacers. The exact mass of each compound is 249.0480, and the residue mass is 215.0430.

glutamates, which also occur in coenzymes such as folate and coenzyme F₄₂₀ with the number of glutamates varying among different organisms.^{17–20} As observed with the previously characterized MF-b, the γ -carboxy terminus of the first glutamate residue is bound to the amino group of the tyramine. This orientation of the γ -linked L-glutamates is opposite from the orientation of the γ -linked L-glutamates found in folates where the glutamate amino group forms a amide bond to the carboxyl group of pterioic acid.²¹ In the case of coenzyme F₄₂₀, the glutamates are also added by the condensation of a carboxylic acid group present in F₄₂₀-0 or F₄₂₀-1 with the amino group of glutamate.²² For sarcinapterin (methanopterin with an

α -linked glutamate) and F₄₂₀-3, the glutamate is added to the α -carboxylate of the core coenzyme structure, analogous to the situation for some folates containing α -linked polyglutamates.^{23–25} MF differs from these other coenzymes, however, because the first γ -linked glutamate is coupled to an amino group attached to the core of the cofactor with the γ -linkages arising from subsequent activation of the glutamate γ -carboxyl for coupling (Figure 1). Recently, our laboratory identified and characterized an ATP-grasp enzyme from *M. jannaschii* that catalyzes the addition the first glutamate residue to tyramine to generate γ -glutamyl-tyramine.³⁴ The enzymes that catalyze the addition of the remaining glutamates for MF-d and MF-e biosynthesis and the addition of the N-(3-carboxy-2- or 3-hydroxy-1-oxopropyl)-L-aspartic acid moiety for MF-e biosynthesis have yet to be identified.

Possible Biosynthesis and Role of Acetyl-methanofuran.

The discovery of acetyl-MF in these methanogens is surprising and intriguing. The presence or proposed existence of acetylated-MF has never been reported. Importantly, acetyl-MF was present at concentrations significantly higher than those of formyl-MF in *Mc. maripaludis* and *Mc. vannielii* (8 and 16% of the total MF-e, respectively), suggesting that it must be an active form of the coenzyme in these cells.

Formyl-methanofuran dehydrogenase from methanogenic archaea catalyzes the reversible conversion of CO₂ and MF to formyl-MF, which is an intermediate in methanogenesis from CO₂.⁴ The first step in this process is the reaction of the amine of MF with CO₂ to form *N*-carboxy-MF (carbamate) that is then reduced by the enzyme to formyl-MF. Such a reaction cannot occur for the formation of acetyl-MF because the formation of a carbamate is not possible with acetate as a substrate. The acetyl-MF would have to be formed either by the biochemical methylation of formyl-MF (Figure 11A) or by the addition of acetate to MF likely through activation by ATP or transfer from acetyl-CoA (Figure 11B). The methylation of formyl-MF is not a known reaction, but it could occur by a sequence of reactions analogous to those seen for acetyl-CoA synthase. For autotrophic growth from C-1 compounds in methanogens, acetyl groups are synthesized as acetyl-CoA by acetyl-CoA decarbonylase/synthase (ACDS) from a CH₃ group and CO.²⁶ In this reaction, CO is derived from CO₂ and the CH₃ group is from methyl-tetrahydrosarcinapterin via a corrinoid-containing methyltransferase protein. Instead of CO being supplied by CO dehydrogenase, it is possible that formyl-MF can supply the CO for the reaction and acetyl-MF is generated instead of acetyl-CoA (Figure 12). Alternatively, another enzyme unrelated to ACDS could catalyze the addition of a methyl group to formyl-MF. Because \bullet CONH₂ and \bullet COOCH₃ radicals have been observed,^{27,28} a plausible

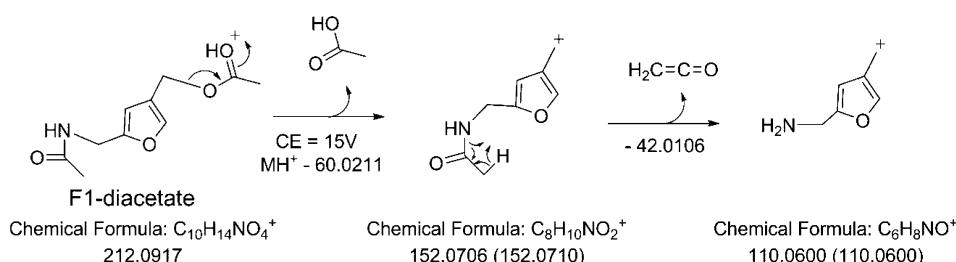


Figure 10. Calculated masses (observed masses) and structures of fragments observed from chemically synthesized F1-diacetate, which match the fragments derived from acetyl-MF.

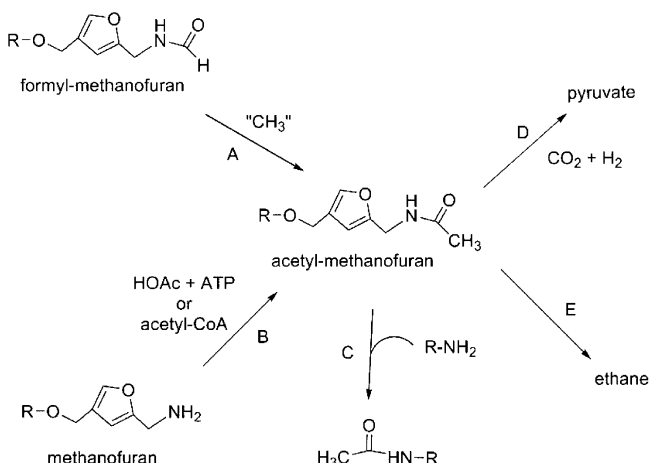


Figure 11. Possible routes for the formation and uses of acetyl-MF.

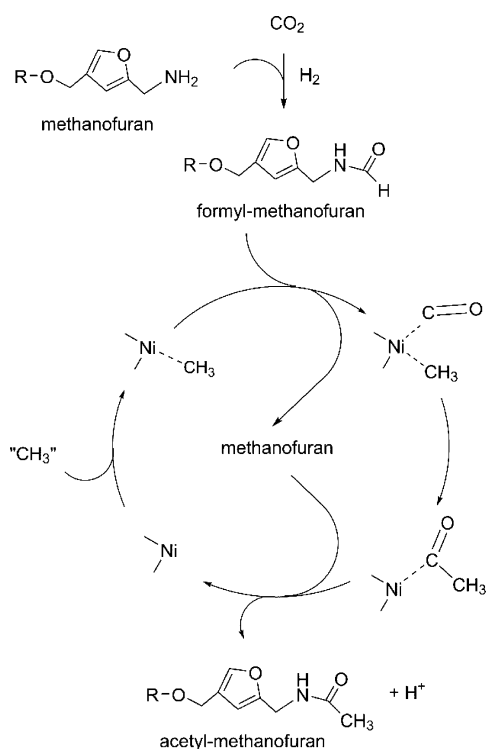


Figure 12. Possible synthesis of acetyl-MF using a cycle analogous to the known pathway for acetyl-CoA synthesis in methanogens.

mechanism would involve radical-dependent methylation. Genomes of methanogens encode many radical S-adenosyl-L-methionine (SAM) superfamily enzymes²⁹ with unknown functions. Radical SAM methyltransferases are widespread and catalyze the methylation of a diverse array of substrates,³⁰ so one of these may catalyze the methylation of formyl-MF to produce acetyl-MF.

Once synthesized, the acetyl-MF could be used to acetylate amines (Figure 11C) or generate pyruvate (Figure 11D). Pyruvate is generated in methanogens through reductive carboxylation of acetyl-CoA catalyzed by pyruvate ferredoxin oxidoreductase (pyruvate synthase).^{31,32} However, it is possible that acetyl-MF is used for pyruvate biosynthesis catalyzed by an as-yet-undiscovered enzyme. Alternatively, the acetyl-MF could be used to transfer its acetate group completely through methanogenesis with the production of ethane as the last step

(Figure 11E). It has been demonstrated that *Msc. barkeri* can produce ethane when grown on H₂/CO₂ when ethanol is added to the medium.³³ These authors proposed that the ethanol was converted to ethane using the terminal portion of the methanol-to-methane pathway, indicating that at least a portion of the methanogenic pathway can use a two-carbon unit. Another possible scenario is that acetyl-MF serves a regulatory role in which the coenzyme is acetylated to decrease the amount of free MF available for CO₂ reduction and thus decrease the level of methanogenesis under specific environmental conditions or in specific growth states. Future experiments looking at the proportions of formyl-MF, acetyl-MF, and free MF in these methanogens grown under different conditions are necessary to address some of these questions. Further studies of the function and biosynthesis of acetyl-MF will reveal new biochemistry present in methanogenic metabolism.

■ AUTHOR INFORMATION

Corresponding Author

*Department of Biochemistry (0308), Room 103, Engel Hall, Virginia Polytechnic Institute and State University, Blacksburg, VA 24061. E-mail: rhwhite@vt.edu. Phone: (540) 231-6605. Fax: (540) 231-9070.

Funding

This study was supported by National Science Foundation Grant MCB1120346 to R.H.W.

Notes

The authors declare no competing financial interest.

■ ACKNOWLEDGMENTS

We thank Dr. Walter Niehaus and Dr. Yu Wang for insightful discussions, Kim Harich for mass spectral assistance, and Dr. W. Keith Ray for obtaining the high-resolution mass spectrometry data. The mass spectrometry resources are maintained by the Virginia Polytechnic Institute and State University Mass Spectrometry Incubator, a facility operated in part through funding by the Fralin Life Science Institute at Virginia Polytechnic Institute and State University and by the Agricultural Experiment Station Hatch Program (CRIS Project VA-135981).

■ ABBREVIATIONS

MF, methanofuran; APMF- γ -Glu₂, 4-[N-(γ -L-glutamyl- γ -L-glutamyl)-p-(β -aminoethyl)phenoxyethyl]-2-(aminomethyl)furan; DCO, 4,5-dicarboxyoctanedioic acid; GC-MS, gas chromatography-mass spectrometry; TM, trifluoroacetyl methyl ester; LC-HR-MS, liquid chromatography-high-resolution mass spectrometry; PDA, photodiode array detector; LC-UV-MS, liquid chromatography-ultraviolet-visible spectrophotometry-mass spectrometry; F1, 5-(aminomethyl)-3-furanmethanol; NBD-F, 4-fluoro-7-nitrobenzofuran; FDAA, 1-fluoro-2,4-dinitrophenyl-5-L-alanine amide; TIC, total ion current; CID, collision-induced dissociation; APMF, [(β -aminoethyl)phenoxyethyl]-2-(aminomethyl)furan; ACDS, acetyl-CoA decarbonylase/synthase; SAM, S-adenosyl-L-methionine.

■ REFERENCES

- Leigh, J. A., and Wolfe, R. S. (1983) Carbon dioxide reduction factor and methanopterin, two coenzymes required for CO₂ reduction

to methane by extracts of *Methanobacterium*. *J. Biol. Chem.* 258, 7536–7540.

(2) Leigh, J. A., Rinehart, K. L., and Wolfe, R. S. (1984) Structure of Methanofuran, the Carbon-Dioxide Reduction Factor of *Methanobacterium thermoautotrophicum*. *J. Am. Chem. Soc.* 106, 3636–3640.

(3) Leigh, J. A., Rinehart, K. L., Jr., and Wolfe, R. S. (1985) Methanofuran (carbon dioxide reduction factor), a formyl carrier in methane production from carbon dioxide in *Methanobacterium*. *Biochemistry* 24, 995–999.

(4) Vorholt, J. A., and Thauer, R. K. (1997) The active species of 'CO₂' utilized by formylmethanofuran dehydrogenase from methanogenic Archaea. *Eur. J. Biochem.* 248, 919–924.

(5) Marx, C. J., Miller, J. A., Chistoserdova, L., and Lidstrom, M. E. (2004) Multiple formaldehyde oxidation/detoxification pathways in *Burkholderia fungorum* LB400. *J. Bacteriol.* 186, 2173–2178.

(6) Pomper, B. K., and Vorholt, J. A. (2001) Characterization of the formyltransferase from *Methylobacterium extorquens* AM1. *Eur. J. Biochem.* 268, 4769–4775.

(7) Jones, W. J., Donnelly, M. I., and Wolfe, R. S. (1985) Evidence of a common pathway of carbon dioxide reduction to methane in methanogens. *J. Bacteriol.* 163, 126–131.

(8) Bobik, T. A., Donnelly, M. I., Rinehart, K. L., Jr., and Wolfe, R. S. (1987) Structure of a methanofuran derivative found in cell extracts of *Methanoscincina barkeri*. *Arch. Biochem. Biophys.* 254, 430–436.

(9) White, R. H. (1988) Structural Diversity among Methanofurans from Different Methanogenic Bacteria. *J. Bacteriol.* 170, 4594–4597.

(10) White, R. H. (1988) Biosynthesis of the 2-(aminomethyl)-4-(hydroxymethyl)furan subunit of methanofuran. *Biochemistry* 27, 4415–4420.

(11) Mukhopadhyay, B., Johnson, E. F., and Wolfe, R. S. (1999) Reactor-scale cultivation of the hyperthermophilic methanarchaeon *Methanococcus jannaschii* to high cell densities. *Appl. Environ. Microbiol.* 65, 5059–5065.

(12) Lin, W., and Whitman, W. B. (2004) The importance of porE and porF in the anabolic pyruvate oxidoreductase of *Methanococcus maripaludis*. *Arch. Microbiol.* 181, 68–73.

(13) Jones, J. B., and Stadtman, T. C. (1977) *Methanococcus vannielii*: Culture and Effects of Selenium and Tungsten on Growth. *J. Bacteriol.* 130, 1404–1406.

(14) Miller, D., Wang, Y., Xu, H., Harich, K., and White, R. H. (2014) Biosynthesis of the 5-(Aminomethyl)-3-furanmethanol Moiety of Methanofuran. *Biochemistry* 53, 4635–4647.

(15) Nagata, Y., Yamamoto, K., and Shimojo, T. (1992) Determination of D- and L-amino acids in mouse kidney by high-performance liquid chromatography. *J. Chromatogr.* 575, 147–152.

(16) Galivan, J., Ryan, T. J., Chave, K., Rhee, M., Yao, R., and Yin, D. (2000) Glutamyl hydrolase. Pharmacological role and enzymatic characterization. *Pharmacol. Ther.* 85, 207–215.

(17) Bair, T. B., Isabelle, D. W., and Daniels, L. (2001) Structures of coenzyme F(420) in *Mycobacterium* species. *Arch. Microbiol.* 176, 37–43.

(18) Forouhar, F., Abashidze, M., Xu, H., Grochowski, L. L., Seetharaman, J., Hussain, M., Kuzin, A., Chen, Y., Zhou, W., Xiao, R., Acton, T. B., Montelione, G. T., Galinier, A., White, R. H., and Tong, L. (2008) Molecular insights into the biosynthesis of the F420 coenzyme. *J. Biol. Chem.* 283, 11832–11840.

(19) Isabelle, D., Simpson, D. R., and Daniels, L. (2002) Large-scale production of coenzyme F420-5,6 by using *Mycobacterium smegmatis*. *Appl. Environ. Microbiol.* 68, 5750–5755.

(20) Osborne, C. B., Lowe, K. E., and Shane, B. (1993) Regulation of folate and one-carbon metabolism in mammalian cells. I. Folate metabolism in Chinese hamster ovary cells expressing *Escherichia coli* or human folylpoly- γ -glutamate synthetase activity. *J. Biol. Chem.* 268, 21657–21664.

(21) Semb, J., Boothe, J. H., Angier, R. B., Waller, C. W., Mowat, J. H., Hutchings, B. L., and SubbaRow, Y. (1949) Pteroic Acid Derivatives. V. Pteroyl- α -glutamyl- α -glutamylglutamic Acid, Pteroyl- γ -glutamyl- α -glutamylglutamic Acid, Pteroyl- α -glutamyl- γ -glutamylglutamic Acid. *J. Am. Chem. Soc.* 71, 2310–2315.

(22) Li, H., Graupner, M., Xu, H., and White, R. H. (2003) CofE catalyzes the addition of two glutamates to F₄₂₀-O in F₄₂₀ coenzyme biosynthesis in *Methanococcus jannaschii*. *Biochemistry* 42, 9771–9778.

(23) Grochowski, L. L., and White, R. H. (2010) Biosynthesis of the Methanogenic Coenzymes. *Comprehensive Natural Products II Chemistry and Biology* 7, 711–748.

(24) Ferone, R., Hanlon, M. H., Singer, S. C., and Hunt, D. F. (1986) α -Carboxyl-linked glutamates in the folylpolyglutamates of *Escherichia coli*. *J. Biol. Chem.* 261, 16356–16362.

(25) Ferone, R., Singer, S. C., and Hunt, D. F. (1986) In vitro synthesis of α -carboxyl-linked folylpolyglutamates by an enzyme preparation from *Escherichia coli*. *J. Biol. Chem.* 261, 16363–16371.

(26) Ferry, J. G. (2010) How to make a living by exhaling methane. *Annu. Rev. Microbiol.* 64, 453–473.

(27) Munoz, F., Schuchmann, M. N., Olbrich, G., and von Sonntag, C. (2000) Common intermediates in the OH-radical-induced oxidation of cyanide and formamide. *J. Chem. Soc., Perkin Trans. 2* 4, 655–659.

(28) Sevilla, M. D., Becker, D., Sevilla, C. L., and Swarts, S. (1985) Reactions of the Methyl and Ethyl Formate Cation Radicals: Deuterium-Isotope Effects. *J. Phys. Chem.* 89, 633–636.

(29) Sofia, H. J., Chen, G., Hetzler, B. G., Reyes-Spindola, J. F., and Miller, N. E. (2001) Radical SAM, a novel protein superfamily linking unresolved steps in familiar biosynthetic pathways with radical mechanisms: Functional characterization using new analysis and information visualization methods. *Nucleic Acids Res.* 29, 1097–1106.

(30) Zhang, Q., van der Donk, W. A., and Liu, W. (2012) Radical-mediated enzymatic methylation: A tale of two SAMS. *Acc. Chem. Res.* 45, 555–564.

(31) Fuchs, G., and Stupperich, E. (1986) Carbon Assimilation Pathways in Archaeabacteria. *Syst. Appl. Microbiol.* 7, 364–369.

(32) Furdui, C., and Ragsdale, S. W. (2000) The role of pyruvate ferredoxin oxidoreductase in pyruvate synthesis during autotrophic growth by the Wood-Ljungdahl pathway. *J. Biol. Chem.* 275, 28494–28499.

(33) Belay, N., and Daniels, L. (1988) Ethane production by *Methanoscincina barkeri* during growth in ethanol supplemented medium. *Antonie Van Leeuwenhoek* 54, 113–125.

(34) Wang, Y., Xu, H., Harich, K. C., and White, R. H. (2014) Identification and Characterization of a Tyramine-Glutamate Ligase (MfnD) Involved in Methanofuran Biosynthesis. *Biochemistry*, DOI: 10.1021/bi500879h.